

A Direct Two-Dimensional Pressure Formulation in Molecular Dynamics

Sumith YD and Shalabh C. Maroo

Department of Mechanical and Aerospace Engineering, Syracuse University, Syracuse, NY 13244, USA.

Two-dimensional (2D) pressure field estimation in molecular dynamics (MD) simulations has been done using three-dimensional (3D) pressure field calculations followed by averaging, which is computationally expensive due to 3D convolutions. In this work, we develop a direct 2D pressure field estimation method which is much faster than 3D methods without losing accuracy. The method is validated with MD simulations on two systems: a liquid film and a cylindrical drop of argon suspended in surrounding vapor.

I. INTRODUCTION

Multiscale coupling of atomistic and continuum simulations is of significant importance in the areas of heat transfer, fracture mechanics and bioengineering [1]. These computations typically map properties determined from atomistic simulations onto grid points in continuum simulations [2]. A very important property is estimation of pressure or stress in the atomistic system, which is used for interfacial energies and surface tension, pressure gradients in fluid simulations and lipid bilayer mechanics. Many simulated systems have inhomogeneity only in two dimensions (2D) such as defect nucleation in bulk and two-dimensional crystals, bio molecular assemblies such as lipid bilayers and membrane proteins, as well as thin film evaporation and heat transfer, and thus only require 2D pressure distribution. However, current literature on local pressure estimation is based on 3D [3] or 1D [4-6] pressure estimation. The 2D pressure distribution is obtained by averaging over the 3D pressure data, and is extremely computationally expensive [7] as it involves a 3D convolution. A generalized method for 3D stress calculations which included temporal averaging weight functions was derived by Yang [8]. Recently, Vanegas [7] and Sanchez et al. [9] applied the modified Hardy versions of IK stress to lipid bilayers, coiled coil protein and graphene sheet to determine continuum level properties from atomistic simulations. Further, there exist a few Irving-Kirkwood versions [10-12] of 1D pressure calculations for 1D inhomogeneous system. However, to the best of our knowledge, no methods are present for a direct 2D pressure estimation. This work presents a 2D pressure estimation algorithm based on Hardy's stress method, which is validated by performing molecular simulations of a suspended liquid film and a cylindrical drop and comparing the results with experimental data and classical Young-Laplace equation, respectively.

Historically, the atomic level virial stresses from statistical analysis were first derived by Irving and Kirkwood [13], now generally referred to as IK method. The need for large ensemble averaging due to the delta function in IK method was circumvented by Hardy in his classical paper [12, 14] by introducing a spreading function and a bond function. The virial stress has two components, a kinetic component and a force component. There existed an ambiguity among researchers about the equivalence of virial stress with Cauchy stress. The ambiguity is thoroughly discussed in Zhou’s paper [15] which claimed that Cauchy stress is not equivalent to virial stress, as the continuum level Cauchy stress is equivalent only to the force component of virial stress. Based on this finding, researchers [16-19] performed a number of molecular studies. Zimmerman [16] showed that, for crystals, Hardy’s stress formulation gave more accurate results than simple local virial averages. A comparative study of different versions of local virial stress was studied by Murdoch [20]. In contrast to Zhou’s work [15], Subramaniyan [21] found that virial stress is indeed the Cauchy stress using specific examples. There were other works [22, 23] which tried to develop the appropriate relation of virial stress and continuum level stresses. Our work also supports that while converting virial stress to a continuum level property, both kinetic component and force component of virial stress should be considered.

II. 2D PRESSURE FORMULATION

The 2D pressure estimation method is developed by reformulating the 3D weight function which significantly reduces the computational cost without losing any desired details in the results. In the 3D method, the modified version of IK stress developed by Hardy [12] has a kinetic component and a virial component. The 3D pressure estimation methodology lies in smearing the kinetic and the virial component into a 3D grid using a weight function and a bond function respectively. The components are smeared into a spherical volume around the particle location. A typical weight function, as used by researchers [8, 22] for 3D grid, is given as:

$$w(r) = C_1[1 - 3r^2/r_s^2 + 2r^3/r_s^3] \quad (1)$$

Specifically, a 3D pressure method requires $N^2 \times N_x \times N_y \times N_z \times N_B$ operations, which can be decreased to $N^2 \times N_x \times N_z \times N_B$ using the outlined 2D pressure method (N is the number of atoms; N_x , N_y and N_z are the number of grid cells along x, y and z-directions respectively; N_B is the number of discrete points for bond function). While extending the pressure estimation theory to a 2D grid, the spherical volume is changed to a cylindrical volume as shown in figure 1a.

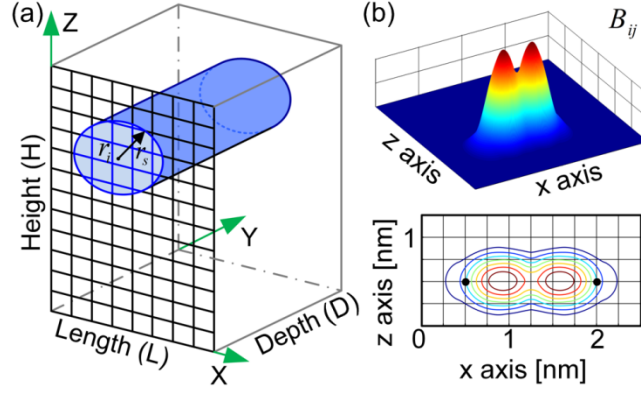


Figure 1. Weight and bond function developed for two-dimensional pressure formulation. (a) Cylindrical volume of influence associated with an atom located at r_i , where r_s is the spread radius, L , D , H are length, depth and height respectively. (b) Visualization of bond function for two atoms separated at a distance of 1.5 nm. The gradient image (lower) shows the surface plot of the same.

The resulting 2D weight function w is (please refer to supporting information for detailed derivation):

$$w(r) = 10[1 - 3r^2/r_s^2 + 2r^3/r_s^3]/(3D \pi r_s^2) \quad (2)$$

where D is the depth of the system along Y (direction of homogeneity) as shown in figure. 1a, r_s is the ‘spread’ radius or the ‘smearing’ radius. Thus, based on the new weight function, the Bond function (B_{ij}), pressure tensor (P), and density of the system (ρ) are defined as:

$$B_{ij}(r_p) = \int_0^1 w(\lambda r_{ij} + r_i - r_p) d\lambda \quad (3)$$

$$P(r_p) = \sum_{i=1}^N m_i v_i \otimes v_i w(r_i - r_p) + \sum_{i=1}^{N-1} \sum_{j=i+1}^N r_{ij} \otimes F_{ij} B_{ij}(r_p) \quad (4)$$

$$\rho(r_p) = \sum_{i=1}^N m_i w(r_i - r_p) \quad (5)$$

where, r_i is the position of i^{th} atom, r_p is the position vector of p^{th} grid point, F_{ij} is the force between two atoms, $r = r_i - r_p$, m_i is the mass of i^{th} atom, v is the velocity and $r_{ij} = r_i - r_j$. Figure 1b shows the variation of bond function for a pair of atoms kept at 1.5 nm apart. The isometric view shows the variation of magnitude of bond function for a spread radius of 0.5 nm. For completeness, we have also derived the 1D variation of pressure and density which is very suitable for 1D inhomogeneous systems like pressure in thin films, lipid bilayers etc. (details can be found in supporting information and is consistent with the derivation of Hardy stress [12]). Additionally formulated 2D forms for some selected functions, along with their 3D functions are included in supporting information. For grid dependent and finite support weight functions like B-splines, a rectangular prism volume should be used instead of cylindrical volume. The computational cost gain from 2D pressure estimation over 3D pressure calculation is also qualitatively discussed in the supporting information.

III. RESULTS AND DISCUSSION

In order to demonstrate and validate the new 2D pressure formulation, we apply it to study the pressure, surface tension and density variations of argon liquid films suspended in argon vapor using molecular dynamics (MD) simulations. In our chosen example (argon liquid film in vapor) and also for lipid bilayer [7], the inhomogeneity is in two dimensions (say, X and Z axes) and there is no density variation along the third dimension (Y axis). The computational domain is shown in figure. 2a. A self-written C++ molecular dynamics code is used for all simulations. The argon liquid film is 10 nm thick with 7.5 nm thick argon vapor on either side along the z -direction. The X - Y cross section size is 5 nm x 5 nm. Periodic boundary conditions are applied in all directions. The vapor and liquid domains in this molecular system are first equilibrated separately [11] for 1000 ps in order to get a stable suspended film and are then integrated. The simulation is run for another 1000 ps on which statistical analysis is performed. The modified Stoddard-Ford LJ potential [24] for argon interactions is used with argon – argon LJ parameters as $\sigma_{Ar-Ar} = 0.34$ nm and $\epsilon_{Ar-Ar} = 1.005841$ kJ/mol. The time step of velocity verlet integration was 5 fs and the thermostat was velocity scaling. A number of simulations for different temperatures, spread radius and cutoff radius were performed. Using the developed 2D formulation, the temporally averaged 2D contours of density and pressure at 90 K are estimated and shown in figures. 2b and 2c. The density and pressure results are compared with the saturation properties from NIST thermodynamic properties database [25] and found to be in very good agreement, which highlights the accuracy of the pressure and density calculation in the new formulation (discussed later in detail).

In a series of simulations by varying the cutoff radius from 1 nm to 1.8 nm, it is found that the thermodynamic properties of argon is best captured by using a cutoff radius of 1.8 nm or larger. However, considering same cutoff and spread radius limits the freedom of simulating an accurate system with finer local details. Thus, in this work, the dependency between spread radius and cutoff radius has been disconnected which enables us to retain the accuracy of the simulation without introducing any artifacts by choosing a higher cutoff radius. Nevertheless, the spread radius can be adjusted to capture the localized effects as desired.

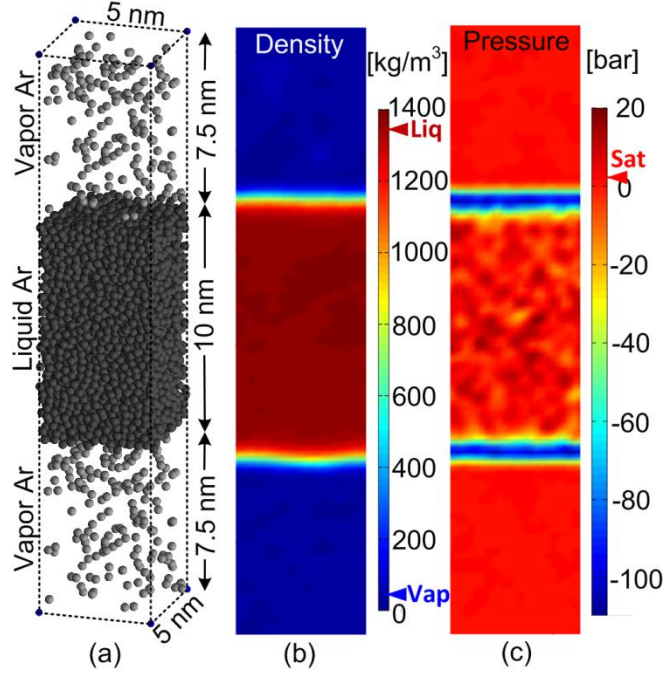


Figure 2. Two-dimensional density and pressure profile in argon multiphase system using the new 2D formulation. (a) A 10 nm thick argon film suspended with 7.5 nm thick vapor on both sides along the z-direction. Two-dimensional (b) density and (c) pressure distribution obtained for the system equilibrated at 90K. The saturation density (NIST data) corresponding to liquid (Liq) and vapor (Vap) are marked in the density plot colorbar, while the saturation pressure (Sat) corresponding to the saturated fluid at 90 K (NIST data) is marked in the pressure plot colorbar showing good agreement with the simulation results.

The sensitivity of spread radius on pressure and density results is studied using the system shown in figure. 2a by varying the spread radius to 0.2 nm, 1 nm and 1.8 nm and estimating the 2D properties of pressure and density. The 2D values are then averaged along the X axis to obtain a 1D pressure and 1D density profile varying along the Z axis as shown in figures. 3a and 3b respectively. Alongside, the pressure and density calculation based on the already-established 1D IK method [11] with a slab thickness of 0.2 nm are also plotted. The results in figures. 3a and 3b show that density and pressure smoothens and spreads to a larger area as the spread radius is increased. Also, when the spread radius is small and comparable to the slab thickness of IK method, both density and pressure matches very well. As expected, the bulk region (vapor only and liquid only) properties are found to be not sensitive to the spread radius since it primarily captures the local effects. Further, to understand the dependency of the bond function to the spread radius, the bond function for two atoms placed at 1.5 nm apart are plotted with varying spread radius of 1 nm, 0.5 nm, 0.3 nm and 0.1 nm (figures. 3c-f). The resulting images show an important result: the spread radius determines the degree of sharpness required to capture the local features as desired. Further, as long as the integral of bond function is unity and conserved, it does not give erroneous values for surface tension, density or pressure. However, care should be taken while selecting the grid cell size for smearing as the results may be less accurate when the

spread radius becomes comparable to grid size (although the resulting artifacts can possibly be alleviated using finite support weight functions like B-Splines).

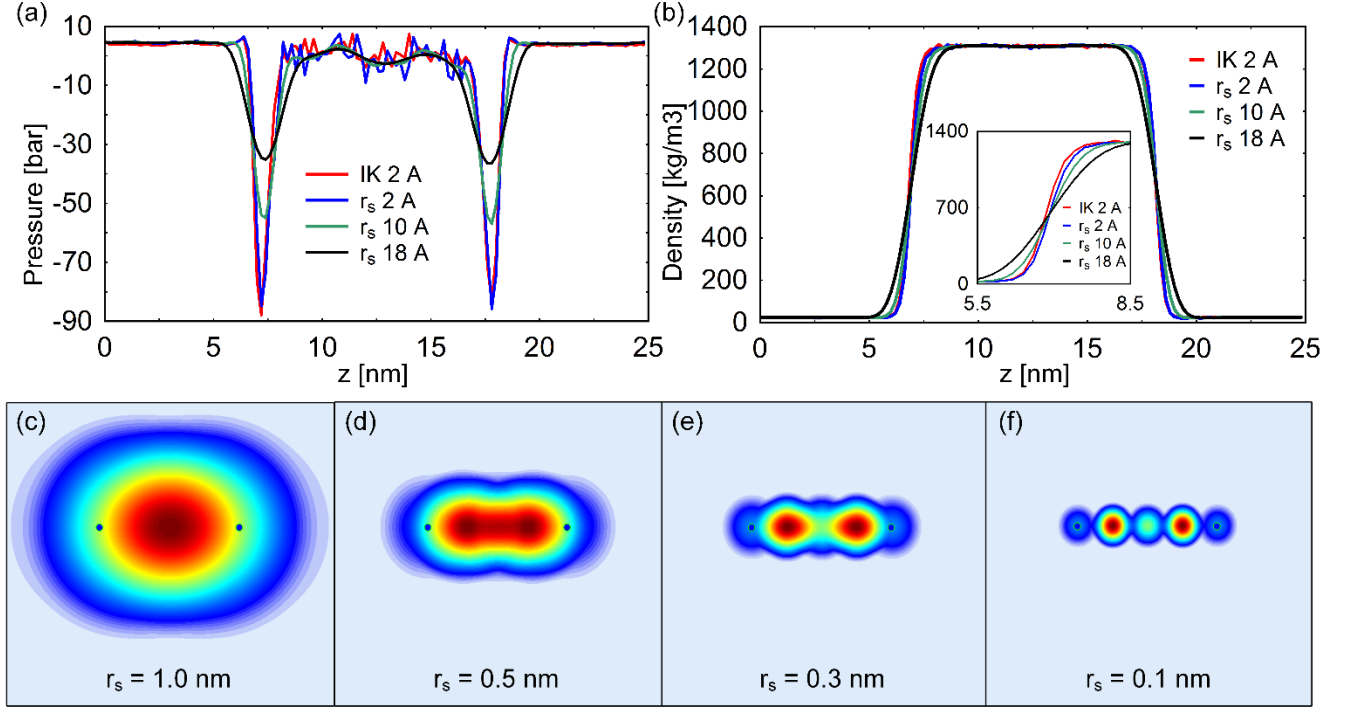


Figure 3. Sensitivity study of spread radius r_s on bond function, pressure and density. (a) Pressure variation across the argon film for different values of r_s . IK 2 A is the case study using the established Irving-Kirkwood’s modified 1D implementation[11] for comparison. The IK 2 A and the new 2D formation based profiles show good agreement when the volume of smearing became comparable. (b) Density variation across the film for different values of r_s which confirms that the overall system bulk properties is not affected by the spread radius. (c-f) Contour plots of bond function with r_s ranging from 1 nm, 0.5 nm, 0.3 nm and 0.1 nm for two atoms kept 1.2 nm apart in a 3 nm x 3 nm domain. The plots visually show how the bond function controls the spreading of the pressure and density across the grids for different spread radii.

Next, we validate the 2D pressure formulation by performing multiple simulations with varying temperature of the argon system (90 K, 100 K, 110 K, 120 K, 130 K, and 140 K) and comparing the simulation results with the experimental thermodynamic properties of argon from NIST database. The spread radius and cutoff radius are chosen as 0.5 nm and 1.8 nm respectively for these simulations. We would like re-emphasize the fact that spread radius does not alter any continuum level quantities and the choice of 0.5 nm as the spread radius is merely arbitrary. Thermodynamic quantities of pressure, density and surface tension are estimated using the developed 2D methodology. The 2D results are averaged along the X axis to obtain a 1D pressure and 1D density profile varying along the Z axis. A visualization of pressure and density variation along the height of the domain is shown in figure. 4a and 4b which is consistent with previous argon film studies [10, 11]. The comparison of

pressure vs. density and surface tension vs. temperature are plotted in figures. 4c and 4d, respectively, and show very good agreement with the experimental data [25].

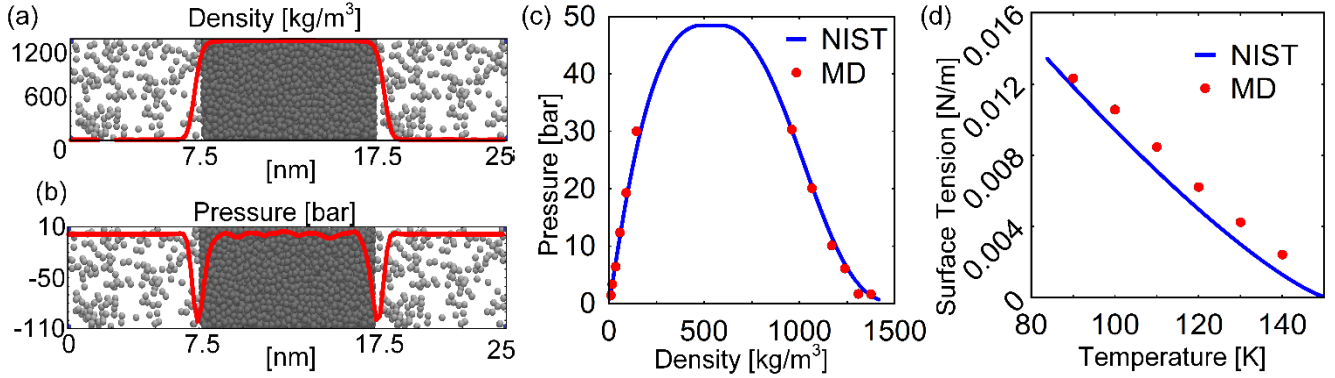


Figure 4. Comparison of MD simulation results with the standard thermodynamic physical data from NIST[25]. (a) 1D density profile and (b) 1D pressure profile, deduced from the new 2D formulation method, plotted over the molecular simulation of argon film. The interface locations capture the expected change in pressure and density. Comparison of MD simulation results and thermodynamic data for (c) pressure vs. density, and (d) surface tension vs. temperature showing excellent agreement. Pressure is estimated by temporal and spatial averaging of vapor and liquid regions separately.

Since the above system is inhomogeneous only in one-dimension, we performed another validation on a curvilinear system which is inhomogeneous in two-dimensions. We estimate the pressure difference in a cylindrical droplet as shown in figure 5a, and compare the result with the classical Young-Laplace equation. The droplet is symmetric in the plane of the figure with a depth of 3 nm and has periodic boundary conditions in all directions with sides of 11 nm each. The droplet is equilibrated for 1000 ps and then production runs are done for another 2000 ps. The pressure and density is estimated every 20 steps and averaged using the method introduced in this work. However, during the course of the simulation, the center of the droplet may vary around the original location. In order to avoid a skewed averaging, center of mass of every data set is found and readjusted to the center of the domain before averaging. The resulting ensemble averaged density and pressure is shown in figures 5b and 5c respectively. The variation of the density and pressure from the center of the droplet towards outside is shown in figures 5d and 5e.

The excess pressure inside the drop is given by the classical Young-Laplace equation:

$$P_{in} - P_{out} = \frac{2\gamma}{R} \quad (6)$$

where P_{out} and P_{in} are the outside and inside pressures of the drop, γ is the surface tension, and R is the radius of the drop. All parameters in equation 6 are estimated independently from the MD simulations. For the system simulated, we obtain $R \sim 2.5 \text{ nm}$

from the density profile, and the surface tension is estimated as $\gamma = 0.00316 \text{ N/m}$ (please see supporting information for the surface tension profile in the droplet). In order to estimate the radial variation of the properties like normal pressure, density, tangential pressure and surface tension, we used the 2D rotation matrix in combination with B-spline interpolation polynomials. The left hand side of equation 6 results in a value of $\sim 3.385 \text{ MPa}$, while the right hand side results in $\sim 2.528 \text{ MPa}$, and thus, is in good agreement with the Young Laplace equation. These simulations confirm the validity and accuracy of the new 2D formulation method developed and presented in this work.

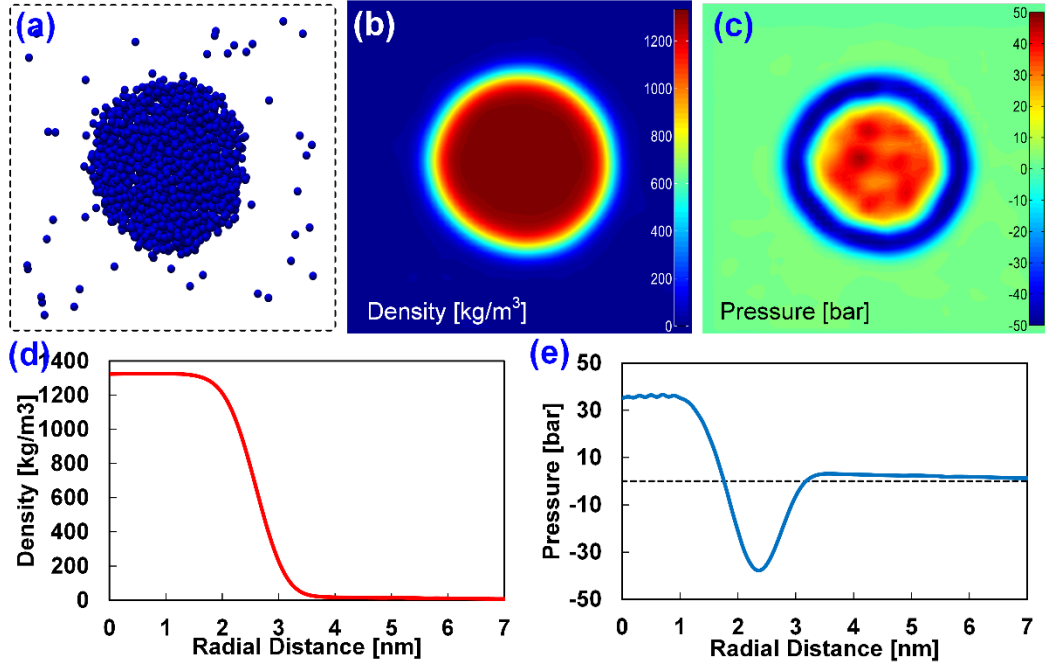


Figure 5. Laplace pressure study in a cylindrical liquid argon droplet. (a) Molecular model of cylindrical argon in a 3d periodic box. (b) Density of the system after ensemble averaging using our 2d method. (c) Pressure of the system ensemble averaged using our 2d method. (d, e) Density and pressure variation from the center of the cylindrical argon radially outward.

IV. CONCLUSIONS

In conclusion, a grid based method for two-dimensional (2D) estimation of pressure and density was developed and validated. The methodology was applied to a suspended argon liquid film in argon vapor with varying temperatures, and results were in very good agreement NIST experimental database values. The method was also applied to the classical problem of pressure difference calculation in a cylindrical drop and the results were found to be in good agreement with the Young Laplace equation. Further, the dependency between spread radius and cutoff radius was disconnected which allows for high accuracy of the simulation by choosing a higher cutoff radius without introducing any artifacts. The spread radius can be adjusted to capture the localized effects in the system as desired. The developed method will be significantly faster (computationally) than

the existing 3D grid method, and can be very useful in determining stresses occurring in lipid bilayers and other systems where inhomogeneity exists only in two of the three dimensions. This work also supports the fact that for the conversion of virial stress to a continuum level property, both kinetic component and force component of virial stress should be considered.

SUPPLEMENTARY MATERIAL

The supplementary material for the derivation of 2D and 1D weight functions, Computational cost associated with 3D and 2D convolutions, Pressure estimation using averaging method, direct estimation of 2D pressure and Laplace pressure estimation for cylindrical drop are discussed in detail in this document.

ACKNOWLEDGEMENTS

This material is based upon work supported by the National Science Foundation under Grant No. 1454450. We acknowledge Prof. Xiantao Li for the helpful discussions and resources.

REFERENCES

- [1] M. F. Horstemeyer, in *Practical Aspects of Computational Chemistry* (Springer, **2010**), pp. 87.
- [2] M. O. Steinhauser, *Computational Multiscale Modeling of Fluids and Solids* (Springer, **2008**).
- [3] O. S. Ollila *et al.*, Physical review letters **102** (**2009**).
- [4] J. Sonne, F. Y. Hansen, and G. H. Peters, The Journal of chemical physics **122** (**2005**).
- [5] E. Lindahl, and O. Edholm, The Journal of Chemical Physics **113** (**2000**).
- [6] D. Heyes *et al.*, The Journal of chemical physics **135** (**2011**).
- [7] J. M. Vanegas, A. Torres-Sánchez, and M. Arroyo, J. Chem. Theory Comput. **10** (**2014**).
- [8] J. Z. Yang, X. Wu, and X. Li, J. Chem. Phys. **137** (**2012**).
- [9] A. Torres-Sánchez, J. M. Vanegas, and M. Arroyo, Phys. Rev. Lett. **114** (**2015**).
- [10] S. H. Lee, Bull. Korean Chem. Soc. **33** (**2012**).
- [11] J.-G. Weng *et al.*, J. Chem. Phys. **113** (**2000**).
- [12] R. J. Hardy, J. Chem. Phys. **76** (**1982**).
- [13] J. Irving, and J. G. Kirkwood, J. Chem. Phys. **18** (**1950**).
- [14] R. J. Hardy, S. Root, and D. R. Swanson, in *AIP Conf. Proc.* (IOP Publishing, **2002**), pp. 363.
- [15] M. Zhou, in *Proc. R. Soc. A* (The Royal Society, **2003**), pp. 2347.
- [16] J. A. Zimmerman *et al.*, Modell. Simul. Mater. Sci. Eng. **12** (**2004**).
- [17] K. Gall, J. Diao, and M. L. Dunn, Nano Lett. **4** (**2004**).
- [18] M. J. Buehler, and H. Gao, Nature **439** (**2006**).
- [19] T. Gates *et al.*, Compos. Sci. Technol. **65** (**2005**).
- [20] A. I. Murdoch, J. Elasticity **88** (**2007**).
- [21] A. K. Subramaniyan, and C. Sun, Int. J. Solids Struct. **45** (**2008**).
- [22] N. C. Admal, and E. B. Tadmor, J. Elasticity **100** (**2010**).
- [23] J. A. Zimmerman, R. E. Jones, and J. A. Templeton, J. Comput. Phys. **229** (**2010**).
- [24] S. D. Stoddard, and J. Ford, Physical Review A **8** (**1973**).
- [25] E. Lemmon, M. McLinden, and D. Friend, NIST chemistry webbook, NIST standard reference database **69** (**2005**).

